

# Solidification behavior and rheo-diecasting microstructure of A356 aluminum alloy prepared by self-inoculation method

Ming Li <sup>1</sup>, \*Yuan-dong Li <sup>1,2</sup>, Xiao-feng Huang <sup>1,2</sup>, Chi Cao <sup>1,2</sup>, and Ying Ma <sup>1,2</sup>

1. State Key Laboratory of Advanced Processing and Recycling of Nonferrous Metals, Lanzhou University of Technology, Lanzhou 730050, China;

2. Key Laboratory of Non-ferrous Metal Alloys and Processing, Ministry of Education, Lanzhou University of Technology, Lanzhou 730050, China

**Abstract:** Semisolid slurry of A356 aluminum alloy was prepared by self-inoculation method, and the microstructure and solidification behavior during rheo-diecasting process were investigated. The results indicate that the semisolid slurry of A356 aluminum alloy can be prepared by self-inoculation method at 600 °C. Primary  $\alpha$ -Al particles with fine and spherical morphologies are uniformly distributed when the isothermal holding time of slurry is 3 min. Liquid phase segregation occurs during rheo-diecasting process of semisolid slurry and the primary particles ( $\alpha_1$ ) show obvious plastic deformation in the area of high stress and low cooling rate. A small amount of dendrites resulting from the relatively low temperature of the shot chamber at the initial stage of secondary solidification are fragmented as they pass through the in-gate during the mould filling process. The amount of dendrite fragments decreases with the increase of filling distance. During the solidification process of the remaining liquid, the nucleation rate of secondary particles ( $\alpha_2$ ) increases with the increase of cooling rate, and the content of Si in secondary particles ( $\alpha_2$ ) are larger than primary particles ( $\alpha_1$ ). With the increase of cooling rate, the content of Si in secondary particles ( $\alpha_2$ ) gradually increases. The morphologies of eutectic Si in different parts of die casting are noticeably different. The low cooling rate in the first filling positions leads to coarse eutectic structures, while the high cooling rate in the post filling positions promotes small and compact eutectic structures.

**Key words:** semisolid; self-inoculation method; secondary solidification; dendrite fragments; primary particles; eutectic structure

CLC numbers: TG146.21

Document code: A

Article ID: 1672-6421(2017)01-001-09

Semisolid metal processing has been widely recognized by experts and scholars since it was first developed, and is regarded as the most promising processing technology in the 21st Century <sup>[1, 2]</sup>. In the semisolid forming process, the remaining liquid phases of alloy can be connected with each other due to the existence of non-dendritic solidification structures in the semisolid slurry, which can effectively reduce or even eliminate solidification shrinkage. Meanwhile, the viscosity of semisolid slurry is higher than liquid, making the gas less involved. Therefore, in theory, using semisolid forming technology can obtain the products

without hole defects <sup>[3-5]</sup>. After more than 40 years of exploration and research, scholars successively developed preparation processes of semisolid microstructure, such as Semi-solid Rheocasting (SSR) <sup>[6]</sup>, Continuous Rheoconversion Process (CRP) <sup>[7]</sup>, New Rheocasting Process (NRC) <sup>[8]</sup>, and Swirled for Equilibration device (SEED) <sup>[9]</sup>, etc. Based on the characteristics of low superheat pouring, liquid-liquid mixed casting, solid-liquid mixed casting, suspension casting and inclined cooling method, a new type of solidification structure control method, self-inoculation method (SIM) <sup>[10]</sup>, is proposed. The process involves mixing liquid alloy with the solid alloy of the same composition (self-inoculants), and subsequently pouring the melt into a mold through a multi-stream fluid director. Heterogeneous nucleation is enhanced due to the addition of self-inoculants (primary inoculation), and large amounts of chilled grains and dendrite fragments are formed in the melt due to the chilling and shearing

## \*Yuan-dong Li

Male, born in 1971, Ph. D, Professor. His research mainly focuses on the semisolid metal processing of nonferrous alloys.

E-mail: liyd\_lut@163.com

Received: 2016-07-19; Accepted: 2016-10-25

of the cooling channel (secondary inoculation), resulting in high grain density and small grain size in solidification structure.

Semisolid metal rheological forming is a direct forming method using solid-liquid mixed slurry with two solidification processes. The process of slurry preparation (solid particles precipitate from liquid alloy) is called primary solidification, and the solidification process of slurry in the subsequent forming (solidification of remaining liquid) is called secondary solidification. In recent years, the study of semisolid metal rheological forming mainly focused on primary solidification, while the research of secondary solidification seldom can be found. Fan et al.<sup>[11]</sup> investigated the shearing effect on solidification characteristics of remaining liquid in A357 aluminum alloy semisolid slurry, and found that the intensive shearing not only influenced the primary solidification, but also the secondary solidification. Li et al.<sup>[12]</sup> studied the microstructural characteristic and secondary solidification behavior of AZ91D magnesium alloy prepared by thixoforming, and proposed that the secondary solidification process involved three stages: the growth of primary  $\alpha$ -Mg particles, remaining liquid solidified by re-nucleation and growth, and eutectic reaction. Chen et al.<sup>[13]</sup> investigated the secondary solidification behavior of AA8006 alloy prepared by suction casting, and determined that the cooling rate influenced not only the solidification of primary  $\alpha$ -Al dendrite, but also the secondary solidification process of the remaining liquid.

Previous studies have indicated that the solidification of remaining liquid in semisolid slurry has an important influence on the final solidification microstructures and the mechanical properties of the alloy. Therefore, it is necessary to study the precipitation behavior of the secondary particles in the remaining liquid of the slurry, the eutectic reaction, and their microstructural characteristics. Based on the previous research<sup>[14-17]</sup>, a thin-walled discal casting of A356 aluminum alloy was produced combining semisolid slurry preparation by self inoculation method with traditional high-pressure die casting. Microstructures of both primary solidification and secondary solidification in different forming parts were analyzed. The relationship between different filling positions and liquid phase segregation was explored by comparing the morphologies and solid fractions of primary particles in different forming positions. Solidification behavior of remaining liquid in rheo-diecasting of A356 aluminum alloy was elaborated by quantitative analysis of secondary particles and the Si morphologies in different forming positions, in order to provide theoretical reference and technical guidance for rheo-diecasting application of A356 aluminum alloy.

## 1 Experimental procedures

### 1.1 Preparation of self-inoculants

Commercial A356 alloy (Table 1) was melted in a pit-type electric resistance furnace. The melt was degassed by C<sub>2</sub>Cl<sub>6</sub> (1mass% of alloy) at 720 °C, then cooled to 700 °C and poured into a metal mold to obtain metal bars with the size of  $\Phi$ 15

Table 1: Chemical composition of commercial A356 alloy (wt.%)

Si	Mg	Fe	Ti	Cu	Zn	Al
7.06	0.27	0.115	0.097	0.001	0.01	Balance

mm×150 mm. Then the bars were machined into small portions with sizes of about 5 mm×5 mm×5 mm.

### 1.2 Slurry preparation and determination of optimum parameters

Figure 1 shows the schematic diagram of slurry preparation by SIM (self-inoculation method). The fluid director was inclined at 45° with a length of 500 mm. The commercial A356 alloy was melted in an electric resistance furnace, and degassed by C<sub>2</sub>Cl<sub>6</sub> (1mass% of alloy) at 720 °C, then the self-inoculants (5mass% of alloy) were added into the melt at 680 °C and stirred quickly. The mixed melt was collected through the fluid director to the collector to obtain the semisolid slurry. Finally, the prepared slurry was held for a certain time (0 min, 3 min, 5 min and 10 min, respectively) at 600 °C, and then directly poured into cold water to obtain water quenched specimens. Specimens were polished and etched by saturated NaOH aqueous solution. The optimum holding time was determined by measuring the average particle size ( $D=(4A/\pi)^{1/2}$ , where  $A$  is area of the particle) and shape factors [ $F=P^2/(4\pi A)$ , where  $P$  is the perimeter of particle] of primary particles using image analysis software Image-Pro Plus 5.0.

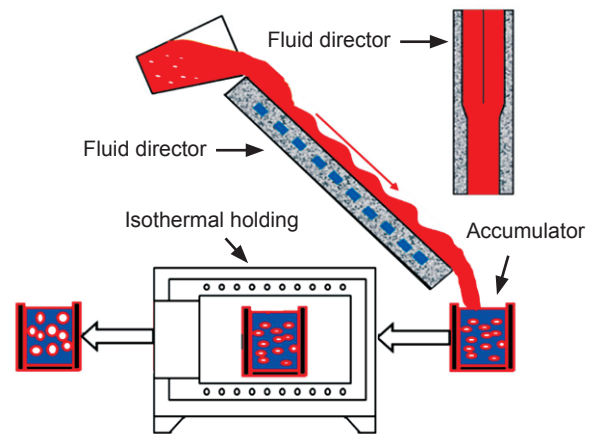
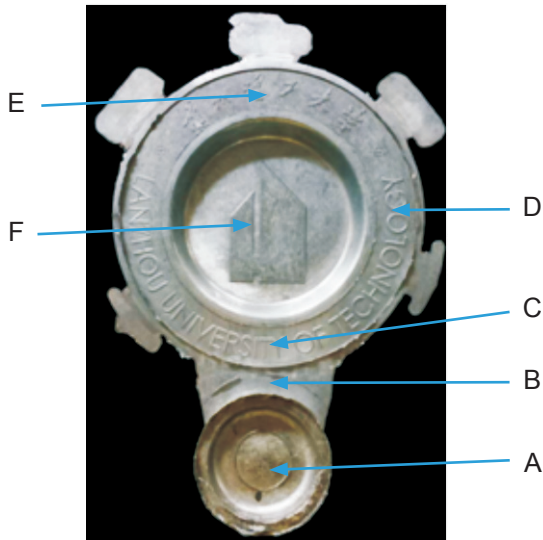


Fig. 1: Schematic diagram of slurry preparation by self-inoculation method

### 1.3 Microstructure observation and quantitative analysis

The re-prepared A356 alloy semisolid slurry under the optimized parameters was chosen to conduct the rheo-diecasting experiment of thin-walled casting using DAK-450 die casting machine. The dies were preheated to 200 °C by hot circulating oil and the shot chamber was preheated to 300 °C. The injection rate was 1.2 m·s<sup>-1</sup> with a pressurization of 160 MPa. A photograph of the die casting with a diameter of 200 mm and a wall thickness of 2 mm is shown in Fig. 2. Forming process and solidification behavior of rheo-diecasting were studied



**Fig. 2: Semi-solid die casting and sampling positions: biscuit (A); in-gate (B); bottom (C); middle (D); top (E) and centre (F)**

by microstructures of different positions shown in Fig. 2. The specimens were prepared by the standard technique of grinding with SiC abrasive paper and polishing with an  $Al_3O_2$  suspension solution, followed by etching in saturated NaOH aqueous solution. The FEG450 scanning electron microscopy (SEM) was carried out with an energy dispersive spectroscopy (EDS) and operated at an accelerating voltage of 3–20 kV to observe the morphologies of secondary particles and eutectic structures.

## 2 Results and discussions

### 2.1 Slurry microstructures under different holding times

Figure 3 shows the water quenched microstructures of A356 aluminum alloy semisolid slurry after holding at 600 °C for 0 min, 3 min, 5 min and 10 min, respectively. It shows that the semisolid slurry of A356 aluminum alloy containing rose-shape and fine dendritic primary particles can be prepared by SIM, as shown in Fig. 3(a). After holding for a short time, the dendritic arms of primary particles are fused, and primary particles become spherical, as shown in Fig. 3(b) and (c). But when the holding time of slurry is too long (such as 10 min), the sizes of the primary particles gradually increase while the merge phenomenon among primary particles becomes obvious, which leads to the appearance of “8” shaped and “spindle-like” structures, as shown in Fig. 3(d).

Figure 4 shows the effect of different holding times on average particle size and shape factor at the same holding temperature (600 °C). It is found that the size of the primary particles increases with the extension of the holding time. The shape factor of the primary particles is close to 1 and the average size is relatively small when the holding time is 3 min. Therefore, the semisolid slurry isothermal holding for 3 min is chosen as the slurry preparation parameter for the semisolid rheo-diecasting experiment.

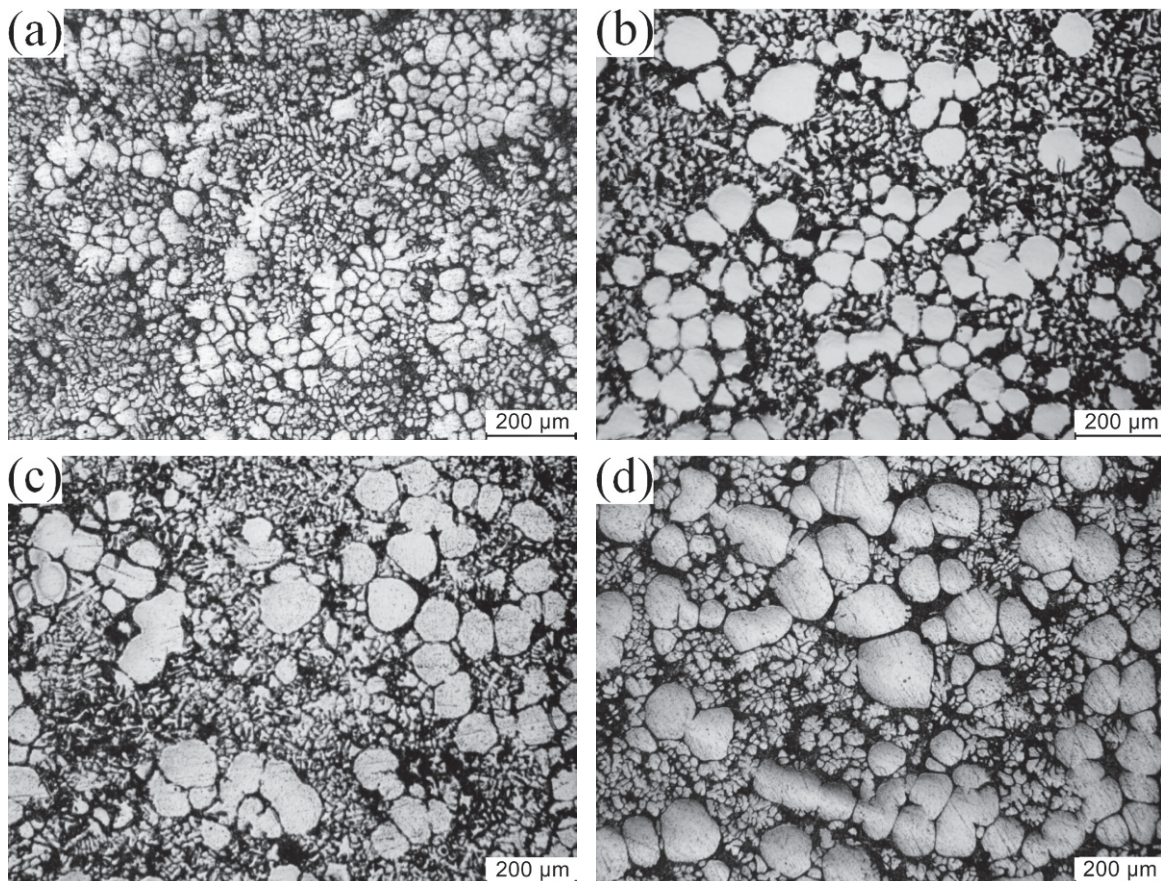


**Fig. 3: Water quenched microstructures of A356 aluminum alloy semisolid slurry at 600 °C for different isothermal holding times: 0 min (a), 3 min (b), 5 min (c), 10 min (d)**

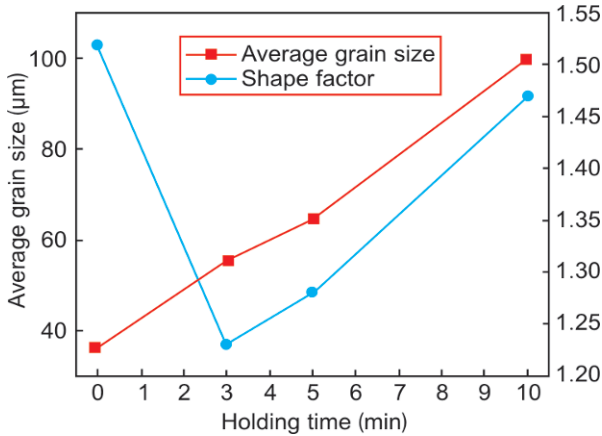


Fig. 4: Curves of shape factor and average particle size during holding process

After adding the self-inoculants, the temperature of the A356 aluminum alloy melt will decrease rapidly. As a result, there will be a large number of high melting points in the local position of the melt, which will be used as the nucleation substrates. When the melt flows through the fluid director, the solidified shell is formed rapidly under the chilled director surface. Subsequently, free grains and dendrite fragments are formed and involved in the melt when the subsequent melt scours and strongly shears the solidified shell, and finally evolves into rose-shape and fine dendritic primary particles. At the end of the director, turbulence occurs when two melt streams are converged, which promotes the thermal field and concentration field of the melt to be uniform. It can be seen from Fig. 3(a) that the water quenched microstructure of semisolid slurry contains rose-shape and fine dendritic primary particles when the slurry is directly poured into the cold water without isothermal holding. During the isothermal holding process, the dendrite roots are fused due to enrichment of the solute, which leads to the formation of single irregular particles, and then the tips of these irregular particles are melted. At the same time, the increased number of particles increases the interfacial energy. Primary particles, as the substrates to absorb solute atoms from liquid phase, are rounded and spherical under the influence of the driving force so that the interfacial energy can be reduced as far as possible. Consequently, primary particles are increased and spheroidized with the extension of isothermal holding time. However, different sizes of original dendrite fragments result in different diameters of spherical primary particles after isothermal holding for a short time. The solute concentration of liquid phase around smaller particles is lower than that around larger particles. With the further extension of the holding time, Si elements will continue to diffuse from large particles to small particles, while the Al elements have the opposite diffusion path. As the result, large particles become larger and small particles become smaller, and even melting and disappearing, which is called Ostwald ripening<sup>[18]</sup>. The “8” shaped and “spindle-like” structures are formed as the intensification of merge phenomenon in the late stage of the isothermal holding process. Therefore, the process of semisolid slurry preparation by SIM can be divided into 3 stages (Fig. 5): (1)

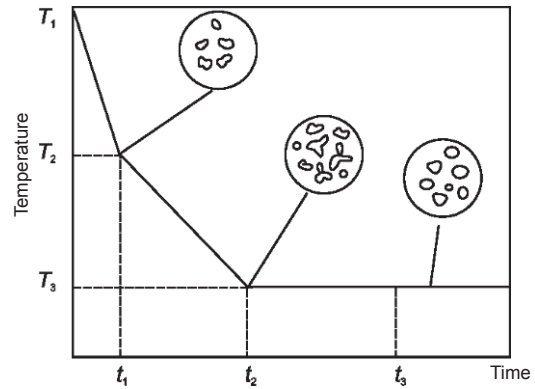


Fig. 5: Stage schematic of spherical particles formation during semisolid slurry preparation by SIM

Precipitation of nucleus by adding self-inoculants into the melt; (2) Formation of large number of nuclei when the melt flows through the fluid director; (3) Spheroidization of primary particles during the isothermal holding process.

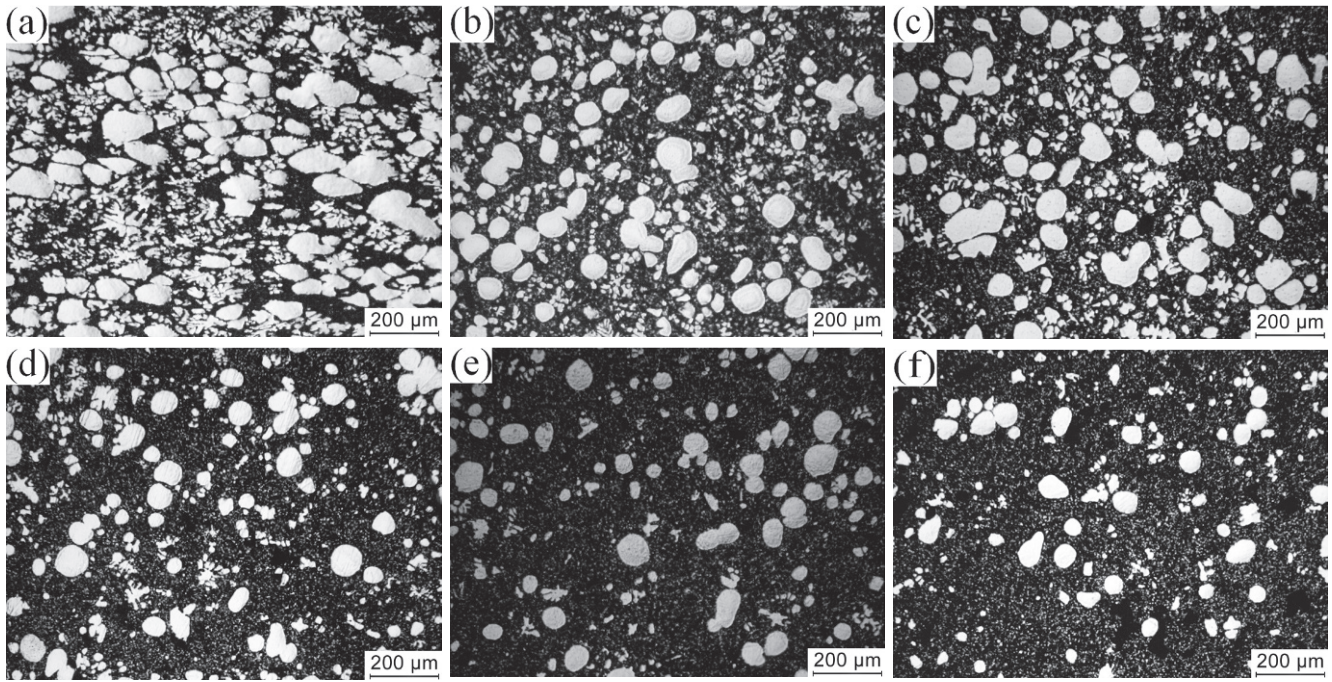
## 2.2 Primary particles ( $\alpha_1$ ) in different positions

Figure 6 shows the microstructures of rheo-diecasting in different positions with the slurry isothermal holding at 600 °C for 3 min. The filling order of semisolid slurry during die casting is from A to F (Fig. 2). It can be seen that the amount of primary particles, average particle size and solid fraction are gradually decreased from A to F.

All the solidification microstructures in different positions are composed of spherical primary particles ( $\alpha_1$ ), secondary particles ( $\alpha_2$ ), some dendrite fragments and eutectic structures. The  $\alpha_1$  particles are uniformly distributed in the solidified structure. The dendrite fragments are formed when pouring the slurry into the shot chamber, and  $\alpha_2$  particles are formed in remaining liquid phase when the slurry is filling the cavity<sup>[11,19]</sup>. It can be seen that the solidification microstructures of A356 aluminum alloy in different positions of die casting are noticeably different. In position A, primary particles have large plastic deformation and bond with each other, and there are a lot of small dendritic crystals around them (Fig. 6a). In position B (Fig. 6b) and position C (Fig. 6c), the majority of primary particles are spherical, with a small number of irregular particles, and the dendrite fragments around the primary particles are smaller than in position A; while in positions D, E and F, primary particles are uniformly distributed and the dendrite fragments around them are fewer and smaller.

In order to further describe the microstructural characteristics in different positions, average particle size, shape factor and solid fraction of the primary particles in different positions are measured, as shown in Table 2. It can be seen that the amount of primary particles, average particle size and solid fraction are gradually decreased from A to F, mainly due to the formation of liquid phase segregation, different cooling rate during the filling process and decreased filling pressure from position A to position F.

It is well known that liquid metal forming mainly depends on the liquid phase flow, while the semisolid metal forming not only



**Fig. 6: Microstructures in different positions of die casting: biscuit, A (a); in-gate, B (b); bottom, C (c); middle, D (d); top, E (e); centre, F (f)**

**Table 2: Average particle size, shape factor and solid fraction of primary particles in different positions of casting**

Position	Number of primary $\alpha_1$	Average particle size ( $\mu\text{m}$ )	Shape factor	Solid fraction (%)
A	72	73.32	1.63	35.6
B	54	63.37	1.36	25.8
C	53	63.17	1.32	24.9
D	40	55.48	1.25	19.9
E	38	55.31	1.23	18.6
F	32	47.83	1.23	10.6

depends on the liquid phase flow but also the solid phase flow and deformation of primary particles in semisolid slurry. The rheological forming process of semisolid slurry includes four kinds of flow mechanisms: liquid phase flow mechanism, liquid-solid phase mixture flow mechanism, slipping mechanism among solid particles and the deformation mechanism of solid phase [20]. In the situation of present work, liquid phase flow mechanism is impossible due to the fast filling speed, and the mainly flow mechanism is liquid-solid phase mixture flow mechanism during the mould filling process. In this experiment, solid fraction is low (about 27%) so that solid particles are dispersed and difficult to contact with each other in the slurry, which makes it difficult to start the slipping mechanism among solid particles during the rheological forming process. However, due to the existence of liquid phase segregation, the amount of solid particles in some areas (such as position A, B and C) are increased, as a result, the slipping mechanism among solid particles can be started. When the filling process is finished, the solidification temperature of position A is higher (because the temperature of the shot chamber is higher than the cavity, and the casting thickness of position A is greater than other positions), where the pressure

is concentrated, so primary particles in this position are easily deformed. Meanwhile, the temperature difference between the shot chamber and dies leads to the different cooling rate in different positions. Namely, the cooling rate from position A to position F is gradually increased due to the heat transfer from high temperature to low temperature. On the other hand, filling pressure is gradually decreased from position A to position F. As a result, it does not have enough driving force for primary particles to overcome viscosity of remaining liquid to fill in position F, showing that the amount of primary particles in position F are the least. The results of the comprehensive role of the above shows that the amount of particles and average particle size of primary particles are gradually decreased from position A to position F (Table 2).

### 2.3 Secondary particles ( $\alpha_2$ ) in different positions

The rheo-diecasting forming by SIM includes two processes: primary solidification process and secondary solidification process. Secondary solidification starts when the semisolid slurry leaves the slurry collector. When the slurry is poured into the shot chamber, heterogeneous nucleation occurs in the remaining liquid and the grains grow into dendrites due to the relatively low temperature of the shot chamber. The dendrites are fragmented when they pass through the narrow in-gate during the mould filling and grow into dendrite fragments (Fig. 6). Different filling distance leads to the different amounts of dendrite fragments. The least number of dendrite fragments are in position F (the center of die casting) due to the longest filling distance, while there are lots of dendrite fragments in positions A, B and C, because the primary particles are gathered in the vicinity of the in-gate, preventing the dendrite fragments from

filling the cavity with liquid phase, and finally gathering in these positions.

Secondary solidification microstructures in different positions of A356 aluminum alloy rheo-diecasting are shown

in Fig. 7. It can be seen that the morphologies of secondary particles are mainly fine spherical and rose shape, except for the microstructure in position A, which has relatively large secondary particles.

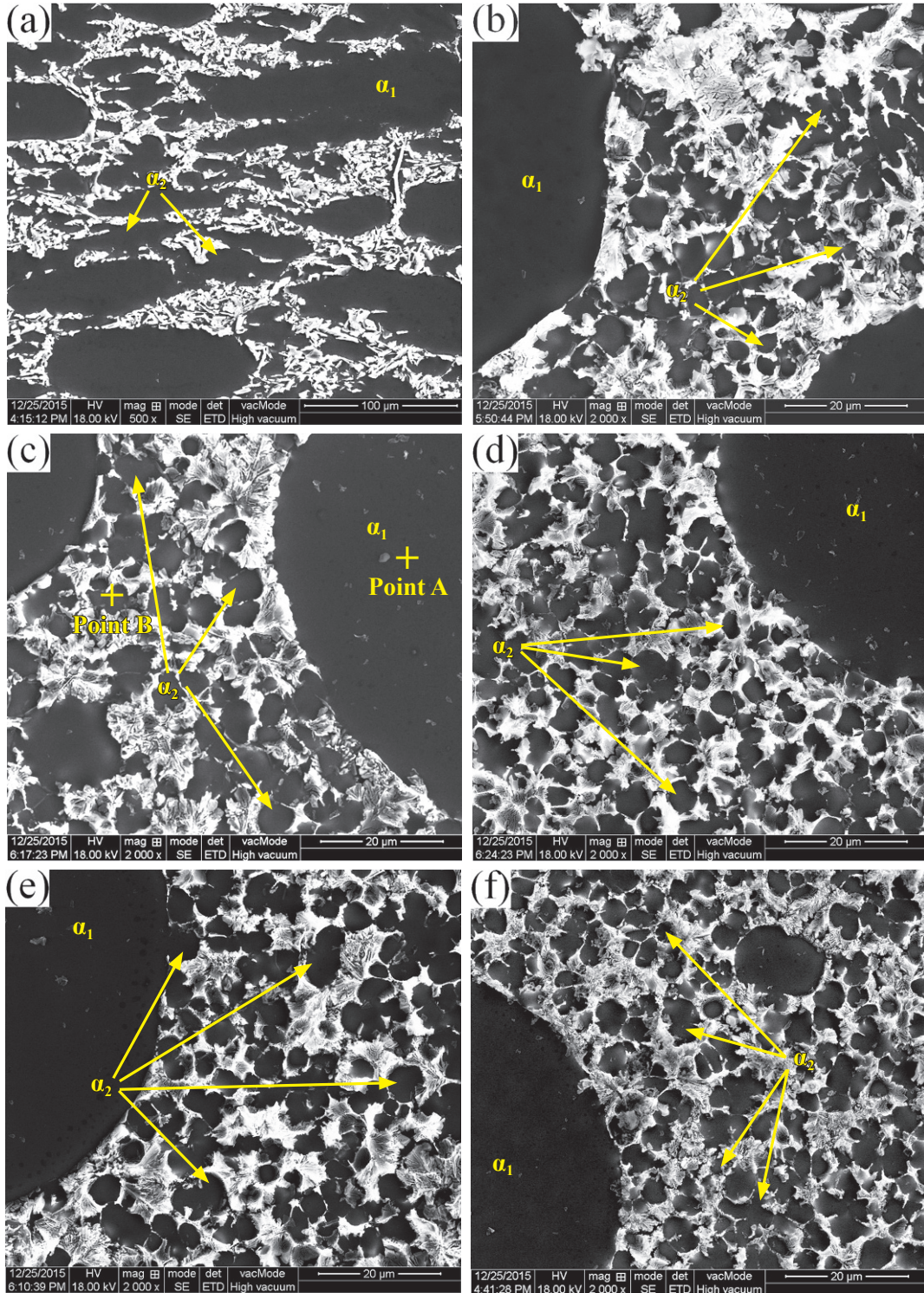


Fig. 7: Second solidification microstructure of rheo-diecasting A356 aluminum alloy in: biscuit, A (a); in-gate, B (b); bottom, C (c); middle, D (d); top, E (e); centre, F (f)

The thickness of the forming part (from position B to F) in this experiment is 2 mm. During the filling process, the semisolid slurry contacts with the cold mould under high pressure, which can provide a large supercooling. The nucleation rate can be

expressed as follows:

$$N = K \exp\left(\frac{-\Delta G}{kT}\right) \bullet \exp\left(\frac{-Q}{kT}\right) \quad (1)$$

where  $K$  is a constant,  $\Delta G$  is the nucleation energy,  $Q$  is the

diffusion activation energy of atoms across the liquid/solid interface,  $k$  is the Boltzmann constant,  $T$  is thermodynamic temperature. For most of the alloy melt, the nucleation rate is increased significantly when the value of relative supercooling is between 0.15–0.25  $T_m$  ( $T_m$  is the melting temperature of alloy), which is called “explosive” nucleation. The melting temperature of A356 aluminum alloy used in this experiment is about 615 °C, while the dies are preheated to 200 °C and the pouring temperature of the alloy is 600 °C, which provides a large enough relative supercooling for “explosive” nucleation. Therefore, nucleation occurs throughout the whole remaining liquid in thin-walled positions (position B to F). In position A, the thickness and the diameter of the biscuit are larger (40 mm and 80 mm, respectively), which causes most of the nucleation to occur in the area of the surface due to the chilling of the shot chamber. According to the Waterloo G<sup>[22]</sup>, the cooling rate  $R$  satisfies the following equation:

$$R = \frac{h(T - T_0)}{c\rho z} \quad (2)$$

where  $h$  is the heat transfer coefficient,  $T$  is the pouring temperature,  $T_0$  is the mould temperature,  $c$  is the specific heat,  $\rho$  is the density and  $z$  is the thickness of the sample. The value of  $c$  is taken as 900 J·(kg·K)<sup>-1</sup> and  $\rho$  as 2,700 kg·m<sup>-3</sup> for aluminum alloy. The mould temperature is 200 °C and the thickness of the sample is 2 mm. According to Ref. [22,23], the value of  $h$  can reach 1.5×10<sup>4</sup> W·m<sup>-2</sup>·K<sup>-1</sup> for aluminum alloy during the thin-walled die casting process. Substituting the above values into the equation (2), the cooling rate  $R$  can reach 10<sup>3</sup> K·s<sup>-1</sup>. Therefore, the nucleus that formed by “explosive” nucleation will grow into particularly small secondary particles due to the large cooling rate (Fig. 7b to 7f). However, in position A, there are lots of dendrite fragments and primary particles and only a little remaining liquid phase due to the liquid phase segregation, which leads to fewer nuclei in this position. Meanwhile, nucleus and fragments have enough time to grow due to low cooling rate in this position, making particle sizes (primary particles and secondary particles) larger than other positions.

In order to further explain the differences between the primary particles and secondary particles in different positions, component analysis of primary particles and secondary particles are carried out (the measured region as shown in Fig. 7c is similar with point A for primary particles and point B for secondary particles, both are in the center of particles), as shown in Fig. 8. It can be seen that the contents of Si in primary particles is lower than secondary particles no matter in which position. In different positions, the contents of Si in both the primary particles and secondary particles are different. The content of Si in primary particles varied between 1.0 and 1.2 and without obvious regularity, while in secondary particles, the content of Si is gradually increased from position A to position F.

The solid fraction of aluminum alloy A356 at 600 °C is measured to be 27% by Pandat (a thermodynamic calculation software). Assuming that the alloy contains only two kinds of elements, Si and Al (because the contents of other elements are low), the average solid solution of Si in the primary particles is

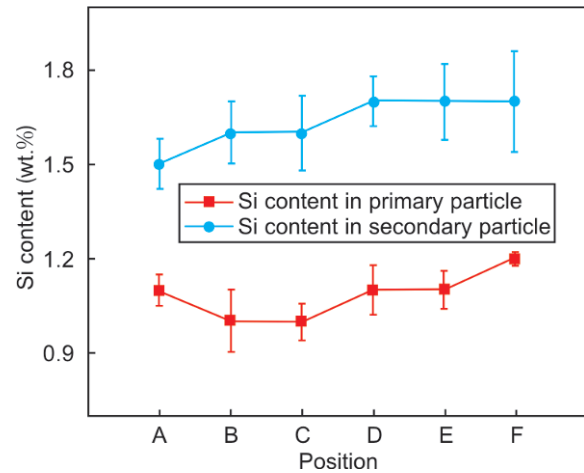


Fig. 8: Content of Si in primary particles and secondary particles in different positions

1.13%, which is measured combining equilibrium phase diagram and Pandat. According to the conservation of mass<sup>[24]</sup>, the composition of the remaining liquid phase,  $C_l$ , can be expressed as:

$$C_l = \frac{C_0 - C_s f}{1 - f} \quad (3)$$

where  $C_0$  is the original content of the alloy,  $f$  is solid fraction and  $C_s$  is the composition of the solid phase. According to equation (3), the content of Al and Si in the remaining liquid phase are 91.7% and 8.3%, respectively, indicating that the composition of the remaining liquid phase are deviated to the eutectic composition (12.6%) compared to the original composition of alloy. The different content of Si between primary particles and secondary particles indicates that primary particles are precipitated in the original composition of the A356 alloy, while secondary particles are formed in the remaining liquid. During the process of die casting, the rapid cooling rate (103 K·s<sup>-1</sup>) causing Si atoms enrichment ahead of the interface and with no time to diffuse, and eventually dissolving in secondary particles. Consequently, the content of Si in secondary particles is higher than primary particles. The calculated value shows that the saturated solid solubility of Si in Al is 1.58%, and the measured content of Si in secondary particles is close to 1.58% (Fig. 8). In position A, the diffusion of Si is sufficient ahead of solid/liquid interface, which leads to lower content of Si in the secondary particles of final solidification microstructure. As the cooling rate increases, the diffusion of Si gradually decreases from position B to position F. As the result, the content of Si is gradually increasing in secondary particles.

## 2.4 Morphologies of eutectic Si in different positions

Figure 9 shows the morphologies of eutectic Si in different positions of die casting. It can be seen that the effect of cooling rate on the morphology of eutectic Si is obvious. As the cooling rate increases from position A to position F, the eutectic structures gradually become more compact. In position A, the eutectic Si has a block structure with the largest size. The eutectic structure in the position B is small strip, and arranged

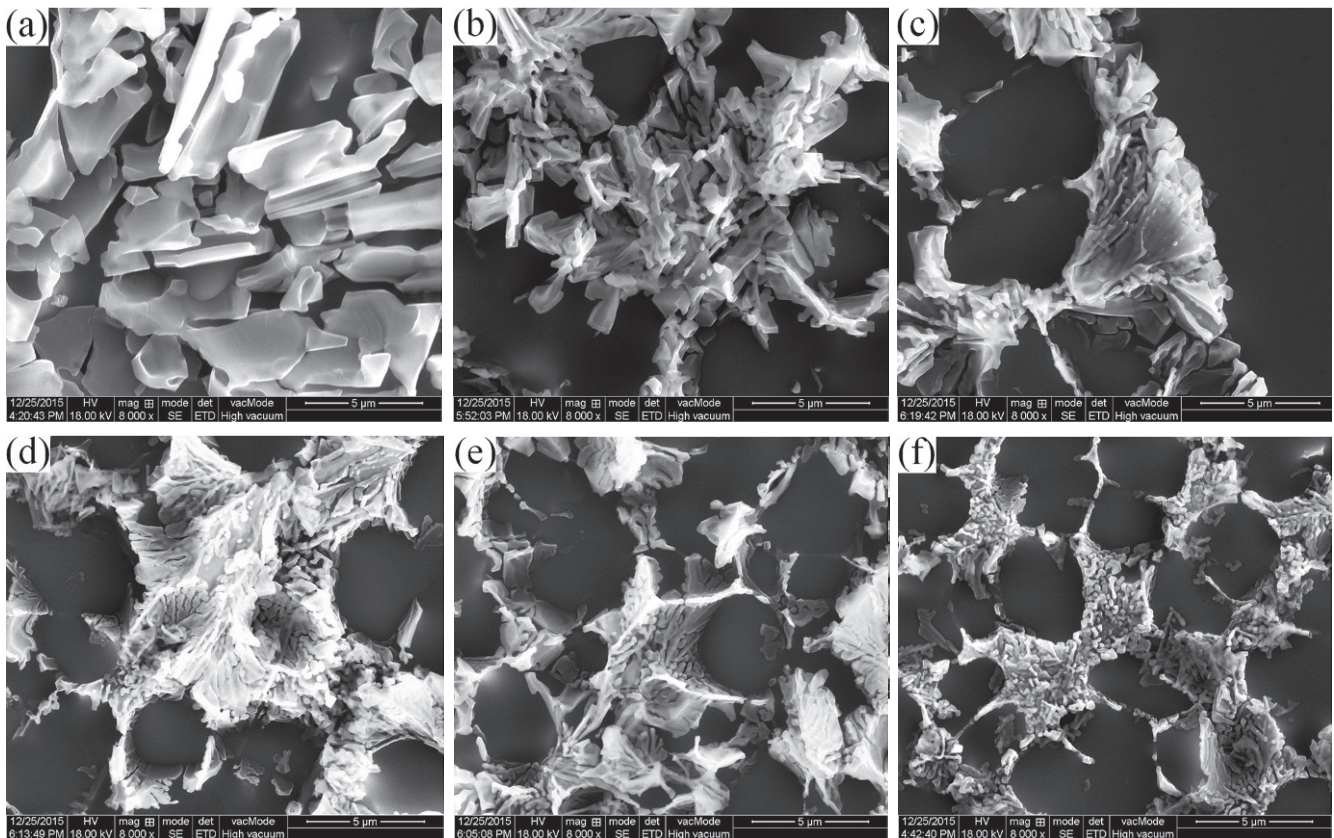


**Fig. 9: Morphology of eutectic structures in different positions of die casting: biscuit, A (a); in-gate, B (b); bottom, C (c); middle, D (d); top, E (e); centre, F (f)**

more closely than position A. In position C, the eutectic structure is small lamellar with transition tendency to fibrous. Most of the eutectic structures are fibrous in position D and E, and there is only a small amount of fine flake, while all the eutectic structures at the center of the die casting (position F) are fine fibrous.

The formation of the intergranular eutectic Si phase between  $\alpha$ -Al particles marks the completion of solidification in the rheo-diecasting process. Si is a faceted phase and Al-Si eutectic is usually considered as an irregular eutectic. The morphology of eutectic silicon in as-cast structure is coarse needle-like, which will seriously affect the performance of the alloy, so it is necessary to obtain a fine eutectic silicon structure to improve the mechanical properties of the products. Usually, modification of the Al-Si eutectic from flake-like to fine fibrous can be achieved by two different ways: by the addition of certain elements (chemical modification) or with a rapid cooling rate (physical modification)<sup>[11]</sup>. In the present study, the eutectic Si in A356 alloy has been found to undergo a morphological change from coarse block-like in position A (Fig. 9a) to fine fibrous in position F (Fig. 9f). This modification of Si morphologies is attributed to the various local cooling rates. In the secondary solidification process of the thin-walled part, the presence of the fine  $\alpha_2$  particles divides the remaining liquid into very small areas. The eutectic reaction involving the formation of the eutectic Si is therefore confined to the small intergranular areas. The high local cooling rate is then able to contribute to the transition of the Si morphology. The higher the local cooling

rate, the more compact the eutectic structure. In position A, the amount of secondary particles is less and their sizes are larger. Due to low cooling rate, eutectic Si has enough time and area to grow into coarse block-like structure. However, eutectic structures are fine with a tight arrangement from position B to position F as the cooling rate gradually increases.

### 3 Conclusions

(1) Semisolid slurry of A356 aluminum alloy can be prepared by Self-Inoculation Method at 600 °C. Primary  $\alpha$ -Al particles with fine and spherical morphology are uniformly distributed when the isothermal holding time of slurry is 3 min.

(2) The solidification microstructures of A356 aluminum alloy in different positions of die casting are noticeably different. Liquid phase segregation occurs during rheo-diecasting forming process of semisolid slurry and the primary particles ( $\alpha_1$ ) have obvious plastic deformation in the area of high stress and low cooling rate.

(3) Small amounts of dendrites result from the relatively low temperature of the shot sleeve at the initial stage of secondary solidification, and then are fragmented as they pass through the in-gate during the die filling process. The amount of dendrite fragments decreases with the increase of filling distance.

(4) During the solidification process of the remaining liquid, the nucleation rate of secondary particles ( $\alpha_2$ ) increases with the increase of cooling rate, and the content of Si in the secondary particles ( $\alpha_2$ ) is greater than primary particles ( $\alpha_1$ ). With the



increase of cooling rate, the contents of Si in the secondary particles ( $\alpha_2$ ) are gradually increasing.

(5) The morphologies of eutectic Si in different parts of die casting are noticeably different. The low cooling rate in the first filling parts leads to coarse eutectic structure, while the high cooling rate in the post filling parts promotes small and compact eutectic structure.

## References

- [1] Flemings M C. Behavior of metal alloys in the semi-solid state. *Metall Trans*, 1991, 22A: 957–981.
- [2] Luo Shoujing, Jiang Yongzheng, Li Yuanfa, et al. Recognition of Semi-Solid Metal forming technologies. *Special Casting and Nonferrous Alloy*, 2012, 32(7): 603–607. (In Chinese)
- [3] Eskin D G, Katgerman S L. Mechanical properties in the semi-solid state and hot tearing of aluminum alloys. *Progress in Materials Science*, 2004, 49(5): 629–711.
- [4] Xu Jun, Zhang Zhifeng. Research Progress of Semisolid Processing Technology. *Journal of Harbing University of Science and Technology*, 2013, 18(2): 1–6.
- [5] Zhao Junwen, Wu Shuseng. Microstructure and mechanical properties of rheo-diecasted A390 alloy. *Transactions of Nonferrous Metals Society of China*, 2010, 20 (S3): s754–s757.
- [6] Yuck J A, Martinez R A, Flemings M C. Development of the semi-solid rheocasting (SSR) process. In: *Proc. of 7th Int. on semi-solid Process of alloys and Composites*, TsukubaJapan, 2002: 659–664.
- [7] Pan Q Y, Findon M, Apelian D. The continuous rheoconversion process (CRP). In: *8th International Conference on Semi-solid Process of Alloys and Composites*, 2004, Limassol, Cyprus.
- [8] Kaudmann H, Mundi A, Potzinger R, et al. An update on the new rheo-casting-development work for Al and Mg alloys. *Die Casting Engineer*, 2002(4): 16–19.
- [9] Midson S P. Rheocasting processes for semi-solid casting of aluminum alloy. *Die Casting Engineer*, 2006, 50(1): 48–51.
- [10] Li Yuandong, Yang Jian, Ma Ying. Effect of pouring temperature on AM60 Mg alloy semi-solid slurry prepared by self-inoculation method ( I ). *Transactions of Nonferrous Metals Society of China*, 2010, 20(6): 1046–1052.
- [11] Hitchcock M, Wang Y, Fan Z. Secondary solidification behaviour of the Al-Si-Mg alloy prepared by the rheo-diecasting process. *Acta Materialia*, 2007, 55(5): 1589–1598.
- [12] Li Yuandong, Chen Tijun, Ma Ying, et al. Microstructural characteristic and secondary solidification behavior of AZ91D alloy prepared by thixoforming. *Transactions of Nonferrous Metals Society of China*, 2008, 18(1): 18–23.
- [13] Chen Zhongwei, Zhang Haifang, Lei Yimin. Secondary Solidification Behaviour of AA8006 Alloy Prepared by Suction Casting. *Journal of Material Science and Technology*, 2011, 27(9): 769–775.
- [14] Xing Bo, Li Yuandong, Ma Ying, et al. Effects of novel self-inoculation method on microstructure of AM60 alloy. *China Foundry*, 2011, 8(1): 121–126.
- [15] Xing Bo, Li Yuandong, Ma Ying, et al. Evolution of rheocast microstructure of AZ31 alloy in semisolid state. *China Foundry*, 2013, 10(4): 221–226.
- [16] Li Yanlei, Li Yuandong, Li Chun, et al. Microstructure characteristics and solidification behavior of wrought aluminum alloy 2024 rheo-diecast with self-inoculation method. *China Foundry*, 2012, 9(4): 328–336.
- [17] Li Yuandong, Zhang Xinlong, Ma Ying, et al. Effect of mixing rate and temperature on primary Si phase of hypereutectic Al-20Si alloy during controlled diffusion solidification (CDS) process. *China Foundry*, 2015, 12(3):173–179.
- [18] Voorhees P W, Hardy S C. Ostwald ripening in a system with a high volume fraction of coarsening phase. *Metallurgical Transactions A*, 1988, 19(11): 2713–2721.
- [19] Ji S, Ma Q, Fan Z. Semisolid Processing Characteristics of AM Series Mg Alloys by Rheo-Diecasting. *Metallurgical and Materials Transactions A*, 2006, 37: 779–787.
- [20] Chen C P, Tsao C Y. Semi-solid deformation of non-dendritic structure - I. phenomenological behavior. *Acta Mater*, 1997, 45(5): 1955–1968.
- [21] Hu Gengxiang, Cai Xun, Rong Yonghua. *Fundamentals of Materials Science*. Shanghai Jiao Tong University Press, Shanghai, China: 2015, 5.
- [22] Waterloo G, Jones H. Microstructure and thermal stability of melt-spun Al-Nd and Al-Ce alloy ribbons. *Journal of Materials Science*, 1996(31): 2301–2310.
- [23] Guo Zhipeng, Xiong Shoumei. Effects of alloy materials and process parameters on the heat transfer coefficient at metal/die interface in high pressure die casting. *Acta Metallurgica Sinica*, 2008, 44(4): 433–439.
- [24] Yang W, Liu F, Wang H F, et al. Non-equilibrium transformation kinetics and primary grain size distribution in the rapid solidification of Fe-B hypereutectic alloy. *Journal of Alloys and Compounds*, 2011(509): 2903–2908.

This research was financially supported by the National Natural Science Foundation of China (No. 51464031).